대한영상의학회지

Magnetic Resonance Enhancement Patterns at the Different Ages of Symptomatic Osteoporotic Vertebral Compression Fractures
유증상 골다공증성 척추 압박 골절에서 골절 시기에 따른 자기공명영상의 조영증강 유형

Ja Yeon You, MD, Joon Woo Lee, MD, Jung Eun Kim, MD, Heung Sik Kang, MD

Department of Radiology, Seoul National University Bundang Hospital, Seongnam, Korea

Purpose: To investigate the magnetic resonance (MR) enhancement patterns of symptomatic osteoporotic vertebral compression fracture (VCF) according to the fracture age, based on the successful single-level percutaneous vertebroplasty (PVP) cases.
Materials and Methods: The study included 135 patients who underwent contrast-enhanced MR imaging and successful PVP from 2005 to 2010 due to a single-level osteoporotic VCF. Two radiologists blinded to the fracture age evaluated the MR enhancement patterns in consensus. The MR enhancement patterns were classified according to the enhancing proportion to the vertebral height and the presence or extent of a non-enhancing cleft within the enhancing area on sagittal plane. The Fisher' exact test, Kruskal-Wallis test and Mann-Whitney U test were performed to assess the differences in the MR enhancement patterns according to the fracture age.
Results: Symptomatic VCFs show variable MR enhancement patterns in all fracture ages. A diffuse enhancing area can be seen in not only the hyperacute and acute VCFs but also the chronic symptomatic VCFs. Symptomatic VCFs having a segmental enhancing area were all included in the hyperacute or acute stage. Most symptomatic osteoporotic VCFs had a non-enhancing cleft in the enhanced vertebral body (128/135, 94.8%). There was no statistical difference of the enhancement pattern according to the fracture age.
Conclusion: Symptomatic VCFs show variable MR enhancement patterns in all fracture ages. The most common pattern is a non-enhancing cleft within a diffuse enhanced vertebra.

INTRODUCTION

The cases of osteoporotic vertebral compression fracture (VCF) have rapidly increased with the rise of the elderly population (1, 2). Recently, percutaneous vertebroplasty (PVP) has been widely used to manage back pain and improve the mobility of the osteoporotic VCF patients (3, 4). However, it is often difficult to determine the symptomatic level in the osteoporotic VCF patients because of the recurrent episodes and the multilevel involvement. Most of the elderly with osteoporotic VCF also have other diseases causing back pain, such as spinal stenosis, degen-

erative change and spinal disc herniation. Conventional radiography and CT are helpful to detect VCF but often fail to determine the symptomatic level in patients with vague symptoms and multiple compression deformities (5, 6). Magnetic resonance (MR) imaging has become an important tool for the evaluation of symptomatic osteoporotic VCF and the preoperative planning of PVP. However, most previous studies have evaluated the MR imaging in osteoporotic VCF by focusing only on the extent of edema on the T1-weighted, T2-weighted and fat-suppressed T2-weighted images (6, 7).

For considering PVP in osteoporotic VCF at our institute, for

several years, we have routinely added the contrast-enhanced fat-suppressed T1-weighted sagittal images to detect marrow edema easily and differentiate osteoporotic VCF from the malignant or infective vertebral collapse, because it is indistinguishable especially in the acute phase (1, 8-10). In our experience, some cases have shown different enhancement patterns of multiple osteoporotic VCFs in the same patient. In these patients, it can be somewhat difficult to know which level of VCF is a recent fracture, causing the new-onset back pain. Hence, we wanted to determine the relations between the MR enhancement pattern and the fracture age of symptomatic VCF. However, few studies have examined the MR enhancement patterns in benign osteoporotic VCF according to the exact fracture age thus far. We hypothesized that if we selected the patients who had symptom improvement after PVP for a single-level VCF, we could conclude that the level of VCF was the cause of the symptoms. Moreover, if we investigated the MR enhancement pattern of that level of VCF in these patients, we could obtain information about the MR enhancement patterns of symptomatic osteoporotic VCF according to the fracture age.

The purpose of our study was to investigate the MR enhancement patterns of symptomatic osteoporotic VCF according to fracture age, based on the successful single-level PVP cases.

MATERIALS AND METHODS

Patient Selection

The institutional review board approved this retrospective study and waived the requirement of obtaining the written informed consent. The study group comprised 406 consecutive patients who underwent PVP performed by an experienced musculoskeletal radiologist in the institutional radiology department from Jan 2005 to Dec 2010. The medical records and imaging studies of these patients were screened by another radiologist to select the successful PVP for the single-level osteoporotic VCF. The inclusion criteria were as follows: 1) presence of contrast-enhanced MR imaging before PVP; 2) PVP for a osteoporotic VCF; 3) successful outcome after the single-level PVP; 4) clear onset time of back pain demonstrated on the medical records. A successful outcome was defined as a reduction in the visual analog scale score of more than 50% on the chart documentation after PVP. From our electronic medical database, 242

patients were excluded for the following: patients who underwent only a non-enhanced MR imaging or simple radiography before PVP (n = 98); patients who confirmed pathologic compression fractures (n = 19); patients who had been performed multi-level PVP in one session (n = 120); and patients who had ineffective outcome after PVP (n = 5) or inadequate medical record on the definite onset time (n = 29). Finally, 135 patients (M : F = 32 : 103, mean age = 75.2 ± 8.4 years; age range 51-96 years) were enrolled in our study. The baseline clinical information (i.e., age, sex), the interval between the onset time of back pain and MR imaging, and the VCF level were recorded for each patient.

MR Protocol

MR was performed at 1.5 T (Gyroscan Intera; Philips, Best, Netherlands), according to the standard protocol at our institution. The T1-weighted, T2-weighted, and contrast enhanced fat-suppressed T1-weighted images were obtained in both sagittal and axial planes with 4-mm slice section thickness. The field of view of sagittal and axial planes was 320 × 320 mm and 170 × 170 mm. The T1-weighted spin-echo sequence was obtained with a repetition time (TR)/echo time (TE) of 400-750/8-22 msec for sagittal and axial planes. The T2-weighted spin-echo sequence was obtained with TR/TE of 2500-4000/100-120 msec for sagittal plane and with TR/TE of 3000-9500/100 msec for axial plane. The fat-suppressed T1-weighted spin-echo sequence with contrast-enhancement was obtained with TR/TE of 400-650/8-20 msec for sagittal and axial planes, using a non-ionic linear chelates gadodiamide (Omniscan, GE Healthcare, Princeton, NJ, USA, 2 mL/sec, total 15 mL).

Analysis of Fracture Age and MR Image

VCFs are divided into four different stages according to the fracture age: hyperacute (up to 7 days), acute (from 8 to 30 days), subacute (from 31 to 90 days) and chronic stage (more than 90 days). Two radiologists (15 years and 3 years of experience, respectively), who were blinded to the fracture age, reviewed the MR images in consensus, focusing on the enhancement pattern. We classified the MR enhancement patterns of symptomatic osteoporotic VCF according to the enhancing proportion to the total vertebral height and the presence or extent of the non-enhancing cleft within the enhancing area, as seen in the most extensively enhanced sagittal plane of the contrast-enhanced fat-

suppressed T1-weighted imaging. The classification criteria were as follows. Pattern A defined vertebra in which enhancement was present in 50% or more of the vertebral body height, including a non-enhancing cleft in 50% or more of the enhancing area (i.e., a large non-enhancing cleft within diffuse enhancing area). Pattern B defined vertebra in which enhancement was present in 50% or more of the vertebral body height, including a non-enhancing cleft in less than 50% of the enhancing area (i.e., a linear or band-like non-enhancing cleft within diffuse enhancing area). Pattern C defined vertebra in which enhancement was present in 50% or more of the vertebral body height without a non-enhancing cleft (i.e., the absence of or a punctate non-enhancing cleft with diffuse enhancing area). Pattern D defined vertebra in which enhancement was present in less than 50% of the vertebral body height with a non-enhancing cleft of the enhancing area (i.e., a linear or band-like non-enhancing cleft with-

in segmental enhancing area). Pattern E defined vertebra in which enhancement was present in less than 50% of the vertebral body height without a non-enhancing cleft (i.e., absence of non-enhancing cleft within segmental enhancing area). The schematic diagrams and examples are shown in Fig. 1. The presence of intravertebral hypointense signal alteration or fluid-filled gap on T2-weighted sagittal image was also evaluated. Based on the correlation with a non-enhancing cleft on the contrast-enhanced T1-weighted image, the T2-weighted image findings were divided into four types. For type 1, there was well-correlated intravertebral hypointense signal alteration or fluid-filled gap on the T2-weighted image with a non-enhancing cleft on the contrast-enhanced T1-weighted image. For type 2, even though there was a definite non-enhancing cleft on the contrast-enhanced T1-weighted image, there was no correlated intravertebral hypointense signal alteration or fluid-filled gap on the T2-weighted

Table 1. Relation of Different Enhancement Patterns to Fracture Age*

Pattern[+]	Pattern A	Pattern B	Pattern C	Pattern D	Pattern E	Total
Hyperacute	40	19	1	6	1	67
Acute	18	23	1	0	3	45
Subacute	11	6	1	0	0	18
Chronic	3	2	0	0	0	5
Total	72	50	3	6	4	135

Note.—*Fracture age; hyperacute = upto 7 days, acute = from 8 to 30 days, subacute = from 31 to 90 days, chronic = more than 90 days.
[+]Pattern; Pattern A = a large non-enhancing cleft within diffuse enhancing vertebral body, Pattern B = a linear or band-like non-enhancing cleft within diffuse enhancing vertebral body, Pattern C = the absence of or a punctate non-enhancing cleft within diffuse enhancing vertebral body, Pattern D = a linear or band-like non-enhancing cleft within segmental enhancing vertebral body, Pattern E = the absence of non-enhancing cleft within segmental enhancing vertebral body
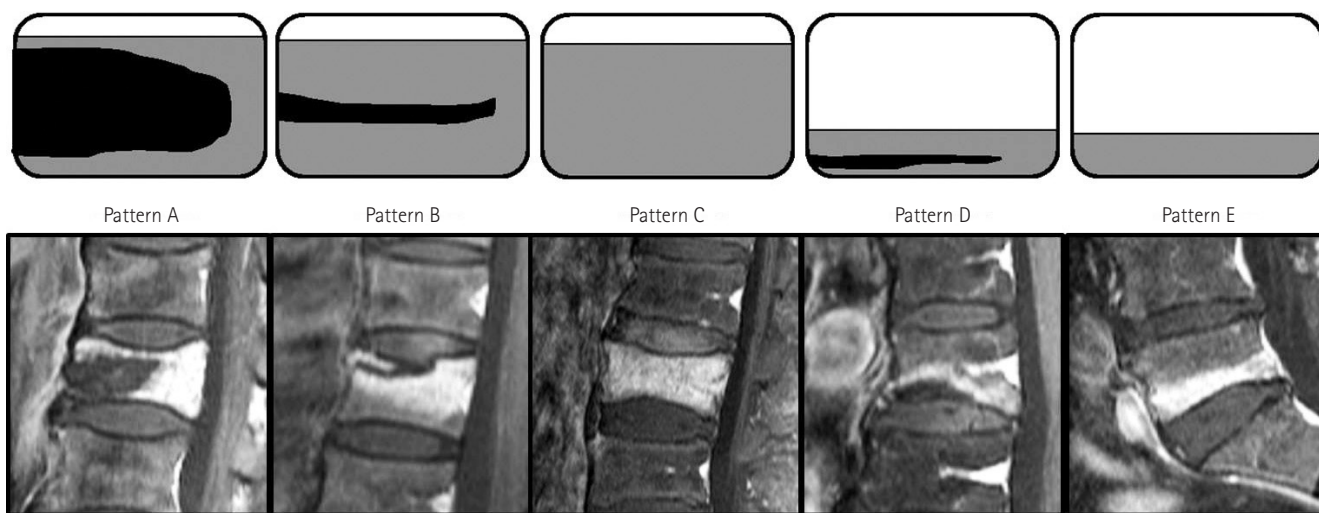

Pattern A   Pattern B   Pattern C   Pattern D   Pattern E

Fig. 1. Schematic diagrams and examples of magnetic resonance enhancement patterns. Pattern A shows a large non-enhancing cleft within diffuse enhancing area. Pattern B shows a linear or band-like non-enhancing cleft within diffuse enhancing area. Pattern C shows the absence of or a punctate non-enhancing cleft within diffuse enhancing area. Pattern D shows a linear or band-like non-enhancing cleft within segmental enhancing area. Pattern E shows the absence of non-enhancing cleft within segmental enhancing area.

image. For type 3, in reverse, there was definite intravertebral hypointense signal alteration or fluid-filled gap on the T2-weighted image without a correlated non-enhancing cleft on the contrast-enhanced T1-weighted image. For type 4, there was neither intravertebral hypointense signal alteration or fluid-filled gap on the T2-weighted image, nor a non-enhancing cleft on the contrast-enhanced T1-weighted image.

Statistical Analysis

The Fisher's exact test was used to analyze the relation between the fracture stage and the MR enhancement pattern. The relationship between the exact fracture age and the MR enhancement pattern were tested by Kruskal-Wallis test. The subgroup analysis according to the presence of diffuse enhancement or internal non-enhancing cleft was done using Man-Whitney U test. Statistical analyses were performed using SPSS, version 17 software (SPSS, Chicago, IL, USA). Statistical significance was assumed at p value less than 0.05.

RESULTS

The interval between trauma or the back pain onset and MR imaging ranged from 0 days to 300 days (mean, 14.7 days). According to the fracture age, 67 patients were assigned to hyperacute stage, 45 patients to acute stage, 18 patients to subacute stage and 5 patients to chronic stage. Most symptomatic VCFs were included in the hyperacute and acute stage (112/135, 82.9%). Only five patients were included in the chronic stage (over 3 months). In patients with symptomatic VCFs, the first lumbar spine was the most commonly involved, and the twelfth thoracic spine was the second most common level.

Correlation with Fracture Age and MR Enhancement Pattern

All osteoporotic VCFs showed enhancement on the contrast-enhanced fat-suppressed T1-weighted imaging. The most frequent enhancement pattern of symptomatic osteoporotic VCFs was Pattern A (72/135, 53.3%) (Table 1). The second most frequent enhancement pattern was Pattern B (50/135, 37.0%). The proportion of Pattern A and B in all fracture ages was over 90% (122/135, 90.3%).

Pattern A was the most common pattern in the hyperacute, subacute and chronic stages. In the acute stage ($n = 45$), Pattern B ($n = 23$, 51.1%) was the most common pattern. Pattern A ($n = 18$, 40.0%) and Pattern E ($n = 3$, 6.7%) in the acute stage were followed in order. Patterns D and E were seen in the hyperacute or acute stage, but were not shown in the subacute and chronic stages.

The Fisher's exact test indicated no significant relation between the fracture stage and the MR enhancement pattern. The Mann-Whitney U test showed that the presence of the diffuse enhancing area or the internal non-enhancing cleft was not significantly associated with exact fracture age. In addition, the Kruskal-Wallis test showed no significant relationship between the exact fracture age and the five enhancement patterns.

Most symptomatic vertebras, except in seven cases (128/135, 94.8%), had at the least a linear or band-like non-enhancing cleft in the enhanced vertebral bodies (i.e., Patterns A, B and D). The non-enhancing clefts on the contrast enhanced T1-weighted image were well-correlated with intravertebral hypointense signal alteration or fluid-filled gaps on the T2-weighted image in 119 patients (88.8%, type 1). In type 1, the non-enhancing clefts were frequently much larger and clearer than intravertebral hypointense signal alteration or fluid-filled gap on the T2-weighted images. Nine patients (6.7%) were included in type 2. There were no cases in type 3. Seven patients (5.2%) with Patterns C and E were all included in type 4.

DISCUSSION

Contrast-enhanced MR imaging has been used to evaluate acute VCFs, especially to discriminate the malignant from benign VCFs, although there are some limitations (9, 11, 12). However, few studies have examined the MR enhancement patterns of benign osteoporotic VCFs according to the fracture age. According to our study, symptomatic VCFs show variable MR enhancement patterns in all fracture ages. We also observed the following interesting results. First, the diffuse enhancing area (in 50% or more of the vertebral body height) can be seen in not only the hyperacute and acute VCFs but also the chronic symptomatic VCFs. Second, symptomatic VCFs having a segmental enhancing area (in less than 50% of the vertebral body height) were all included in the hyperacute or acute stages. Third, most symptomatic osteoporotic VCFs had a non-enhancing cleft in

the enhanced vertebral body.

In our study, the most common enhancement pattern in all fracture ages was the enhancement in 50% or more of the vertebral body height, including the non-enhancing cleft in 50% or more of the enhancing area (Pattern A). The proportion of Patterns A and B (i.e., diffuse enhancing vertebra, including at least a linear or band-like non-enhancing cleft) in all fracture ages was 90.3% (122/135). Thus, the diffuse enhancing area could be seen in not only the hyperacute and acute VCF but also the subacute and even chronic symptomatic VCFs. Previous studies reported that the diffuse enhancement of the vertebral body indicated acute or subacute fracture, presumably representing edema or inflammation (13). The edema in a fractured vertebra is a reactive progressive process that begins after the fracture event, with the increased fluid in the bone (6). It is well-correlated with a high signal intensity in the fat-saturated T2-weighted sequences. As the compression fracture heals, the edema typically resolves along with the patient's pain (14). In our study, patients in the chronic stage showed only Patterns A and B on the contrast enhanced image, because their VCFs were still symptomatic (Fig. 2). Even though the mechanism of the long-lasting bone marrow enhancement in these patients was poorly understood, the continuous enhancement of the bone marrow was well-correlated with the patient's symptoms in our study. Therefore we speculated that the diffuse enhancing area in any stage should be considered the possible symptomatic level, even if it is in the chronic stage.

The patients with VCF, having a segmental enhancing area (Patterns D and E) were all included in the hyperacute and acute stages. It is suspected that the extent of enhancement in VCF is related to the strength of mechanical stress. A segmental enhancing area in VCF is possibly made by a minor trauma, which is quickly recovered. Another possible cause of the segmental enhancing area in VCF in the hyperacute and acute stages is that the MR image was performed too early to see enough inflammation. In the hyperacute or acute stage, a segmental enhancing area can be seen in the symptomatic VCF. Hence, PVP should also be considered in such cases.

Most symptomatic osteoporotic VCFs in our study had at least a linear or band-like non-enhancing cleft in the enhanced vertebral body (i.e., Patterns A, B and D), except for seven cases (128/135, 94.8%). Many authors have reported the internal low signal intensity (emptying gap) of the compressed vertebra as a fluid sign, intravertebral cleft, intravertebral vacuum, Kümmell's disease and so on (13, 15-19). Jung et al. (11) demonstrated that the internal low signal intensity of the compressed vertebra on the T1- and T2-weighted images is a characteristic MR finding in acute osteoporotic VCF. This internal low-signal alteration presumably represents a fracture line or hematoma in the acute phase and the vacuum cavity or nonunion with pseudarthritis in the reparative stage of VCF (6, 15, 20-23). Oka et al. (13) documented that the intravertebral clefts on the T2-weighted images were frequently smaller than the unenhanced area on the contrast-enhanced T1-weighted images. Similarly in our study,
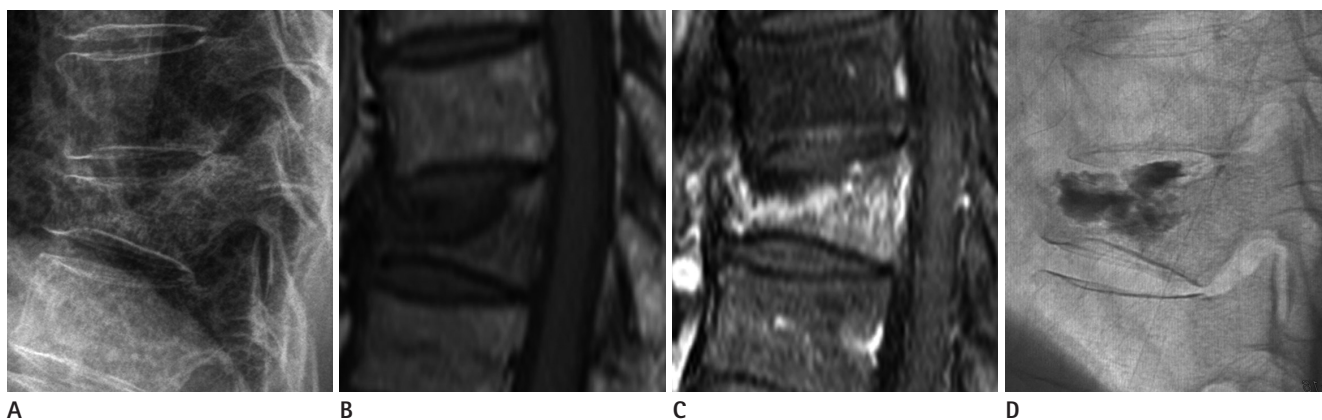

Fig. 2. Imaging in a 73-year woman with chronic symptomatic osteoporotic compression fracture.
A. Lateral radiography obtained 3 month after trauma shows anterosuperior compression fracture of L1 vertebra.
B. T2-weighted image obtained 7 month after lateral radiography **(A)** due to continuous back pain shows hypointense signal alteration in fractured L1 vertebral body.
C. Contrast-enhanced fat-suppressed T1-weighted image shows non-enhancing cleft within diffuse enhanced L1 vertebra (Pattern B).
D. After percutaneous vertebroplasty, chronic back pain of the patient was markedly improved.
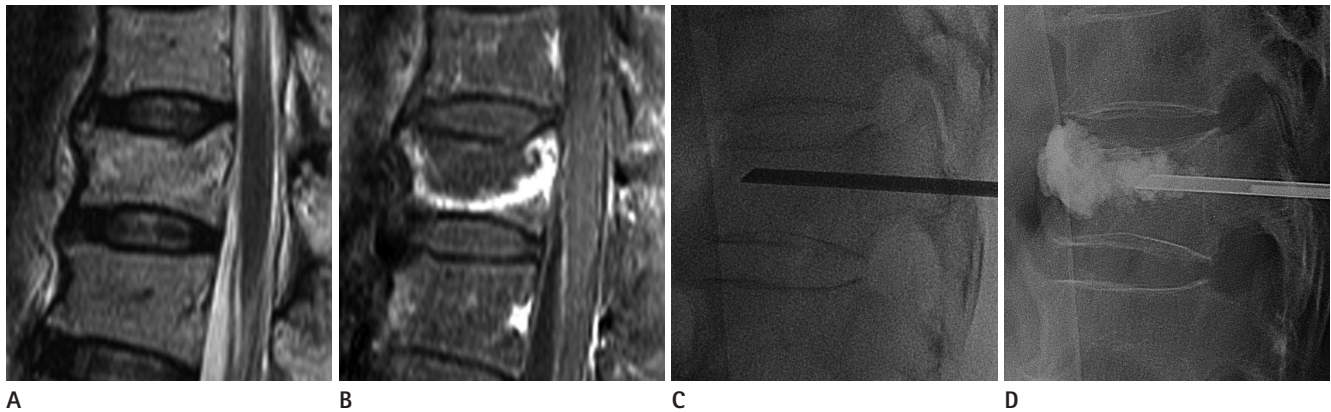
A   B   C   D

Fig. 3. Usefulness of contrast enhanced magnetic resonance (MR) imaging for needle positioning of percutaneous vertebroplasty (PVP). Images in a 63-year-old woman with symptomatic compression fracture of T12 vertebra.
A. On T2-weighted image, there is no demonstrable hypointense signal alteration or fluid-filled gap at T12 vertebra.
B. However, a contrast-enhanced fat-suppressed T1-weighted image shows a large non-enhancing cleft within diffuse enhanced T12 vertebra (Pattern A).
C. On PVP, the vertebroplasty needle tip is placed in the upper third of T12 vertebra, which is well correlated with non-enhancing cleft on contrast enhanced MR image.
D. The bone cement is packing at the non-enhancing cleft of T12 vertebra.

the non-enhancing clefts were much larger and clearer than the intravertebral hypointense signal alteration or fluid-filled gap on the T2-weighted images; hence, we could easily identify them on the contrast-enhanced T1-weighted images. Even the intravertebral hypointense signal alteration was not clearly identified on the T2-weighted image in nine cases with obvious non-enhancing clefts (Fig. 3). We attempted to place the needle in the non-enhancing cleft of the enhanced compressed vertebra during PVP to fill the bone cement at the fracture site first. Several recent investigators underlined that the non-enhancing portion (emptying gap) of VCFs should be completely filled with cement to achieve immobilization and pain relief in PVP (24-27). Oka et al. (13) reported that the unenhanced area of VCF is a reliable sign predicting a solid distribution of the injected cement. Thus, a non-enhancing cleft of osteoporotic VCF on the contrast-enhanced MR imaging may be expected to be a marker of the accurate needle positioning during vertebroplasty, although further investigation is necessary (Fig. 3).

The limitations of our study include its being a retrospective review and the positive selection bias caused by the selection only of patients who have improved symptom after a single-level vertebroplasty. This bias may have artificially decreased the number of patients in groups showing Patterns D and E in our study, because we suspected that their symptoms were not severe enough to receive PVP. However, the selection of patients who underwent the successful single-level vertebroplasty was necessary to clarify whether it was the symptomatic VCF or not. The possibility of recurrent VCF on the same level by unrecognized minor trauma during a follow-up cannot be completely excluded, as our study was based on the medical records.

In conclusion, symptomatic osteoporotic compression fractures show variable MR enhancement patterns in all fracture ages. The most common pattern is a non-enhancing cleft within diffuse enhanced vertebra.

REFERENCES

1. Kallmes DF, Jensen ME. Percutaneous vertebroplasty. *Radiology* 2003;229:27-36

2. Ensrud KE, Thompson DE, Cauley JA, Nevitt MC, Kado DM, Hochberg MC, et al. Prevalent vertebral deformities predict mortality and hospitalization in older women with low bone mass. Fracture Intervention Trial Research Group. *J Am Geriatr Soc* 2000;48:241-249

3. Tanigawa N, Komemushi A, Kariya S, Kojima H, Shomura Y, Ikeda K, et al. Percutaneous vertebroplasty: relationship between vertebral body bone marrow edema pattern on MR images and initial clinical response. *Radiology* 2006; 239:195-200

4. Kobayashi K, Shimoyama K, Nakamura K, Murata K. Percutaneous vertebroplasty immediately relieves pain of osteoporotic vertebral compression fractures and prevents

prolonged immobilization of patients. *Eur Radiol* 2005;15: 360-367

5. Chen WT, Shih TT, Chen RC, Lo SY, Chou CT, Lee JM, et al. Vertebral bone marrow perfusion evaluated with dynamic contrast-enhanced MR imaging: significance of aging and sex. *Radiology* 2001;220:213-218

6. Yamato M, Nishimura G, Kuramochi E, Saiki N, Fujioka M. MR appearance at different ages of osteoporotic compression fractures of the vertebrae. *Radiat Med* 1998;16:329-334

7. Riggs BL, Melton LJ 3rd. The worldwide problem of osteoporosis: insights afforded by epidemiology. *Bone* 1995; 17(5 Suppl):505S-511S

8. Brown DB, Gilula LA, Sehgal M, Shimony JS. Treatment of chronic symptomatic vertebral compression fractures with percutaneous vertebroplasty. *AJR Am J Roentgenol* 2004; 182:319-322

9. Cuénod CA, Laredo JD, Chevret S, Hamze B, Naouri JF, Chapaux X, et al. Acute vertebral collapse due to osteoporosis or malignancy: appearance on unenhanced and gadolinium-enhanced MR images. *Radiology* 1996;199:541-549

10. Shih TT, Huang KM, Li YW. Solitary vertebral collapse: distinction between benign and malignant causes using MR patterns. *J Magn Reson Imaging* 1999;9:635-642

11. Jung HS, Jee WH, McCauley TR, Ha KY, Choi KH. Discrimination of metastatic from acute osteoporotic compression spinal fractures with MR imaging. *Radiographics* 2003;23: 179-187

12. Tan SB, Kozak JA, Mawad ME. The limitations of magnetic resonance imaging in the diagnosis of pathologic vertebral fractures. *Spine (Phila Pa 1976)* 1991;16:919-923

13. Oka M, Matsusako M, Kobayashi N, Uemura A, Numaguchi Y. Intravertebral cleft sign on fat-suppressed contrast-enhanced MR: correlation with cement distribution pattern on percutaneous vertebroplasty. *Acad Radiol* 2005;12: 992-999

14. Layton KF, Thielen KR, Cloft HJ, Kallmes DF. Acute vertebral compression fractures in patients with multiple myeloma: evaluation of vertebral body edema patterns on MR imaging and the implications for vertebroplasty. *AJNR Am J Neuroradiol* 2006;27:1732-1734

15. Baur A, Stäbler A, Arbogast S, Duerr HR, Bartl R, Reiser M. Acute osteoporotic and neoplastic vertebral compression fractures: fluid sign at MR imaging. *Radiology* 2002;225: 730-735

16. Do HM. Magnetic resonance imaging in the evaluation of patients for percutaneous vertebroplasty. *Top Magn Reson Imaging* 2000;11:235-244

17. Dupuy DE, Palmer WE, Rosenthal DI. Vertebral fluid collection associated with vertebral collapse. *AJR Am J Roentgenol* 1996;167:1535-1538

18. Stallmeyer MJ, Zoarski GH, Obuchowski AM. Optimizing patient selection in percutaneous vertebroplasty. *J Vasc Interv Radiol* 2003;14:683-696

19. Kümmel HB. Some meandering rivers of Wisconsin. *Science* 1895;1:714-716

20. Hasegawa K, Homma T, Uchiyama S, Takahashi H. Vertebral pseudarthrosis in the osteoporotic spine. *Spine (Phila Pa 1976)* 1998;23:2201-2206

21. Ito Y, Hasegawa Y, Toda K, Nakahara S. Pathogenesis and diagnosis of delayed vertebral collapse resulting from osteoporotic spinal fracture. *Spine J* 2002;2:101-106

22. Mochida J, Toh E, Chiba M, Nishimura K. Treatment of osteoporotic late collapse of a vertebral body of thoracic and lumbar spine. *J Spinal Disord* 2001;14:393-398

23. Baba H, Maezawa Y, Kamitani K, Furusawa N, Imura S, Tomita K. Osteoporotic vertebral collapse with late neurological complications. *Paraplegia* 1995;33:281-289

24. Lane JI, Maus TP, Wald JT, Thielen KR, Bobra S, Luetmer PH. Intravertebral clefts opacified during vertebroplasty: pathogenesis, technical implications, and prognostic significance. *AJNR Am J Neuroradiol* 2002;23:1642-1646

25. Mathis JM. Percutaneous vertebroplasty: complication avoidance and technique optimization. *AJNR Am J Neuroradiol* 2003;24:1697-1706

26. Peh WC, Gelbart MS, Gilula LA, Peck DD. Percutaneous vertebroplasty: treatment of painful vertebral compression fractures with intraosseous vacuum phenomena. *AJR Am J Roentgenol* 2003;180:1411-1417

27. Kim DY, Lee SH, Jang JS, Chung SK, Lee HY. Intravertebral vacuum phenomenon in osteoporotic compression fracture: report of 67 cases with quantitative evaluation of intravertebral instability. *J Neurosurg* 2004;100(1 Suppl Spine):24-31

유증상 골다공증성 척추 압박 골절에서 골절 시기에 따른 자기공명영상의 조영증강 유형

유자연 · 이준우 · 김정은 · 강흥식

목적: 유증상 골다공증성 척추 압박 골절로 성공적인 경피적 척추성형술을 받은 환자에서 골절시기에 따른 자기공명영상의 조영증강 유형들을 분석하고자 한다.

대상과 방법: 이 연구는 2005년부터 2010년까지 골다공증성 단일 척추 압박 골절로 조영증강 자기공명영상을 시행 후 성공적인 경피적 척추성형술을 받은 135명의 환자를 대상으로 하였다. 골절시기에 대해 눈가림한 두 명의 영상의학과 의사가 의견 합의를 통해 조영증강 자기공명영상을 분석하였다. 조영증강 유형은 시상면에서 척추 높이 대비 조영증강영역의 비율과 조영증강영역 내부의 비조영증강 틈의 존재유무 및 정도에 따라 구분하였다. 골절시기와 조영증강 유형 간의 차이를 알아보기 위해 Fisher' exact test, Kruskal-Wallis test 및 Mann-Whitney U test를 이용하였다.

결과: 미만성 조영증강영역은 초급성과 급성뿐만 아니라 만성 유증상 척추 압박 골절에서도 관찰되었다. 분절성 조영증강영역을 보이는 경우는 모두 초급성기 또는 급성기에 해당되었다. 대부분의 유증상 골다공증성 척추 압박 골절은 조영증강영역 내부에 비조영증강 틈을 가지고 있었다(128/135, 94.8%). 하지만 골절시기에 따라 자기공명영상의 조영증강 유형들 간에 통계학적으로 유의한 차이를 보이지 않았다.

결론: 증상이 있는 척추 압박 골절은 골절시기와 상관 없이 다양한 조영증강 유형을 보인다. 가장 흔한 유형은 미만성 조영증강영역 내부에 비조영증강 틈을 가지고 있는 유형이다.

분당서울대학교병원 영상의학과